

Interfacial Self-Assembly of Cell-like Filamentous Microcapsules**

Dorota I. Rożkiewicz, Benjamin D. Myers, and Samuel I. Stupp*

We report herein the development of a self-assembly method to rapidly produce cell-like, filamentous microcapsules (MCs) that have high surface area and encapsulate liquids or gels. The fibrous surfaces and shell walls of the MCs can be biologically functionalized using bioactive peptide amphiphiles (PAs), and the cores can harbor biopolymers, proteins, and other macromolecules. This novel method combines the spray-based production of nebulized biopolymer microdroplets^[1,2] with the recently reported ultrafast self-assembly of oppositely charged, high-molecular-weight biopolymers and PAs.^[3–5] There are numerous techniques available for microcapsule formation such as interfacial coacervation or interfacial polycondensation,^[6] layer-by-layer (LbL) polyelectrolyte complexation and colloid-templated self-assembly,^[7–13] emulsification with polymer phase separation,^[14–17] spray-drying methods,^[18–20] and microfluidic emulsion droplet formation.^[21–24] The advantage of the method reported herein is the combination of a self-assembly process that leads to structural complexity with the very broad range of bioactivity offered by peptide amphiphiles.

The bioactive filament-forming PAs are composed of a hydrophobic alkyl tail, and a β -sheet-forming peptide domain, followed by peptide sequences with charged amino acids or bioactive epitopes that can either bind to receptors or to specific proteins by design (Figure 1 A).^[25–29] These molecules assemble into high-aspect-ratio filaments upon electrostatic screening of the charged amino acids and the formation of β sheets. Hydrophobic collapse of these filament-forming molecules under strong screening conditions leads to the display of a high density of biological signals on their surfaces (on the order of 10^{15} signals per cm^2).^[25] In vivo and in vitro

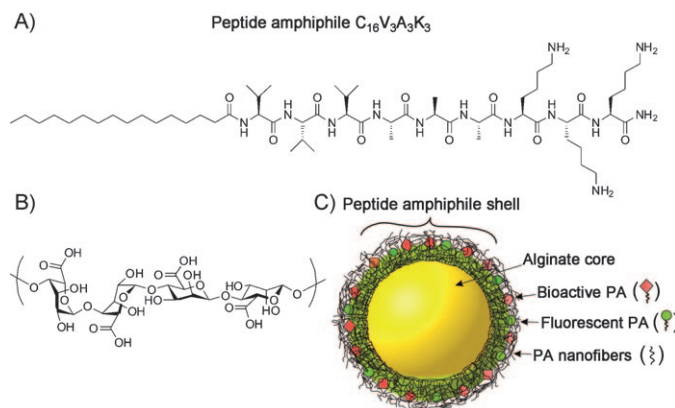


Figure 1. A) Molecular structure of peptide amphiphile $\text{C}_{16}\text{V}_3\text{A}_3\text{K}_3$. B) Alginate. C) Schematic illustration of the cross-section of a PA-alginate microcapsule.

studies have shown that certain PA molecules that bear bioactive epitopes promote regeneration of spinal cord axons, angiogenesis, bone regeneration, cartilage repair, proliferation of bone marrow cells, and selective differentiation of neural progenitor cells into neurons.^[25,26,28–33] We previously demonstrated that solutions of PAs and oppositely charged biopolymers can self-assemble at the liquid–liquid interface to form hierarchically structured membranes that can be permeable to proteins to produce saclike structures on the macroscale with millisecond speeds (with size scales of millimeters).^[3–5] The shells of these sacs are highly structured and their surfaces are fully covered with nanoscale filaments. We have modified this approach for the production of filamentous MCs less than $100\ \mu\text{m}$ in diameter (Figure 1 C). These micrometer-scale objects could be created with highly bioactive properties, high surface area, and dimensions approaching those of cells.

The first step in the MC formation requires generation of picoliter droplets of a biopolymer solution. We built a spray-based device that enables production of droplets with diameters (d_{MC}) as small as $5\ \mu\text{m}$ and an average production rate of 1×10^8 microcapsules per second. The nebulizing device has three components: a) a pressure microinjector for the delivery of a biopolymer solution, b) a glass capillary (orifice diameter ca. $40\ \mu\text{m}$), and c) compressed gas (nitrogen or air; see the Supporting Information). We nebulized the stream of 0.25 wt % aqueous alginate (AL) solution using a high-velocity flow of nitrogen. The microdroplets of the biopolymer solution were directly ejected into a 0.1 wt % aqueous solution of $\text{C}_{16}\text{V}_3\text{A}_3\text{K}_3$ PA (Figure 1 A) to induce the membrane-forming self-assembly process that occurs on the millisecond timescale. After allowing 15 min for dynamic self-assembly between the PA molecules and the biopolymer,^[3]

[*] Prof. S. I. Stupp

Departments of Chemistry, Materials Science and Engineering, and Medicine, and Institute for BioNanotechnology in Medicine Northwestern University, Chicago, IL 60611 (USA)
E-mail: s-stupp@northwestern.edu

Dr. D. I. Rożkiewicz

Institute for BioNanotechnology in Medicine and Department of Chemistry Northwestern University, Chicago, IL 60611 (USA)

B. D. Myers

NUANCE Center, Department of Materials Science and Engineering Northwestern University, Evanston, IL 60208 (USA)

[**] This work was supported by Department of Energy grant DE-FG02-00ER45810. D.I.R. thanks the Netherlands Organisation for Scientific Research (NWO) Rubicon grant, Royal DSM N.V. for stipend support. This work made use of instruments in the NUANCE Center and the Institute for BioNanotechnology in Medicine. The NUANCE Center is supported by NSF-NSEC, NSF-MRSEC, the Keck Foundation, the State of Illinois, and Northwestern University.



Supporting information for this article is available on the WWW under <http://dx.doi.org/10.1002/anie.201100821>.

the MCs were centrifuged and rinsed thoroughly with MilliQ water. This method results in microdroplets that are uniform in size ($d_{MC} \approx 25 \mu\text{m}$) and shape with a coefficient of variation (CV) of approximately 20%. A microfilter (such as a cell strainer) can be inserted into the spraying line to reduce the size range. We have investigated different concentrations of alginate and PA solutions. We found that high concentrations of alginate (e.g., 2 wt%) were difficult to spray because of their high viscosity. This difficulty led to MCs with large sizes, that is, on the order of hundreds of micrometers. On the other hand, low concentrations of alginate ($< 0.25 \text{ wt}\%$) resulted in capsules with a very thin membrane, which led to their rapid fusion during the spraying process. High concentrations of PA (e.g., 2 wt%) led to gel formation and were avoided for MC fabrication. The surface morphology, cross-section, shape, and uniformity of the MCs were investigated with scanning electron microscopy (SEM), focused ion beam (FIB), and optical and fluorescence microscopy. Samples for SEM imaging were prepared by the critical point drying processing (CPD) of the MCs followed by osmium coating. The MCs have filamentous shells with high surface area (Figure 2 A, B). The length of the surface nanofibers can exceed $10 \mu\text{m}$ (Figure 2 B, inset) but on average they are in the range 2–3 μm , with diameters below 20 nm. Based on our previous work,^[3] the orientation of surface fibrils is likely to be related to the diffusion of macromolecules through a diffusion barrier. The thickness of the membrane depends on the incubation time of MCs in the PA solution, which in our case is 15 min, and for the MCs of approximately $25 \mu\text{m}$ in diameter, the wall thickness is approximately 350 nm. Also the PA-MCs can have either a liquid or gel core (Fig-

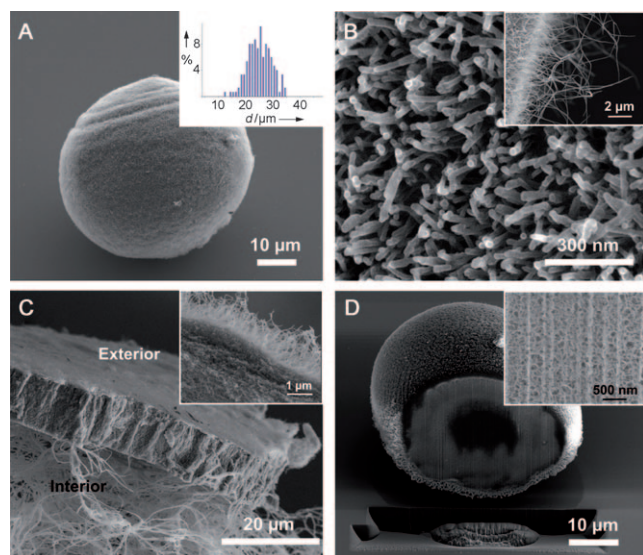


Figure 2. SEM images of A) A PA-AL microcapsule. Inset: MC size distribution graph. B) Top view of nanofibrous surface of the MC. Inset: side view. C) Liquid-core MC (diameter ca. 1 mm) fractured to examine biopolymeric interior. The PA-AL membrane separates the biopolymer liquid core from the exterior. The inset shows a cross section of the capsule membrane. D) Gel-filled MC cross-sectioned by FIB to investigate the morphology of the inner core. Inset: expansion of the cross-linked alginate interior of the MC that comprises a dense, “sponge”-like alginate gel.

ure 2 C, D) formed by cross-linking the alginate with, for example, Ca^{2+} ions either during or after MC formation. Core gelation enables the formation of mechanically stable structures that have resistance to damage during processing (rinsing, centrifuging, and handling) whereas liquid-core capsules are more susceptible to collapse and burst. The gelation process can be reversed by the addition of a chelating agent solution such as sodium citrate. To investigate the interior of liquid-core capsules, we fractured them before SEM imaging (Figure 2 C). From the SEM investigation, we can see an outer layer of entangled filaments. This layer is formed when PA filaments directly contact with an oppositely charged biopolymer to screen electrostatic interactions and trigger self-assembly. Gel-core MCs were prepared by CPD and cross-sectioned by FIB/SEM to study the interior morphology and the structure of the membrane (Figure 2 D). The gel-core capsules have a sponge-like interior structure since the alginate is cross-linked with Ca^{2+} ions to form a dense polymer network and the exterior exhibits nanofibrous morphology.

The ability of the MCs to encapsulate and release proteins and other macromolecules would be obviously important in developing biomedical applications. This possibility was evaluated with UV/Vis spectrometry and fluorescence microscopy using fluorescein isothiocyanate (FITC) labeled dextrans (3–70 kDa) and FITC-labeled bovine serum albumin (BSA). Five different spraying solutions were prepared; each was a mixture of 1 mg mL^{-1} FITC-labeled dextran molecular weight standards (3–5 kDa, 10 kDa, 40 kDa, 70 kDa), FITC-BSA with 0.5 wt% alginate in 1:1 (v/v) ratio. The solutions were sprayed into 0.1 wt% $\text{C}_{16}\text{V}_3\text{A}_3\text{K}_3$ containing 2 wt% CaCl_2 and the resulting MCs were rinsed with H_2O and phosphate-buffered saline (PBS). The encapsulation of dextrans and BSA was investigated with fluorescence microscopy. The FITC-BSA and dextran exhibit strong fluorescence that is uniform across the entire MC (Figure 3 A). For the release studies, the MCs were transferred into the releasing medium (Dulbecco’s PBS, pH 7.4) at 37°C for 24 h. After this time, we

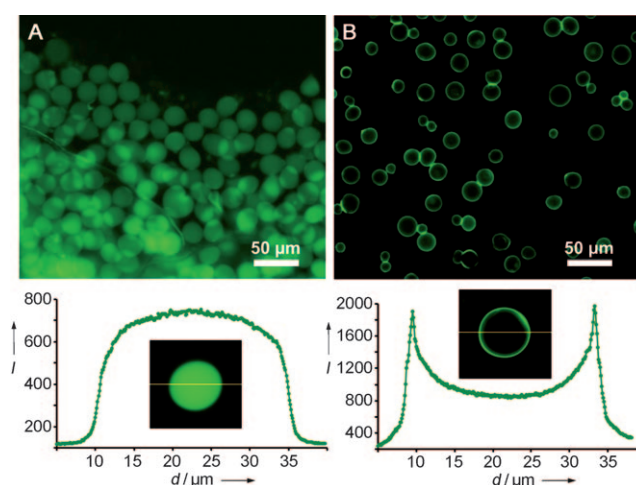


Figure 3. Fluorescence microscopy image and fluorescence intensity profile of PA-AL microcapsules (A) with encapsulated FITC-BSA (B) containing FITC-labeled PA in its shell.

did not observe a fluorescence signal from the MCs. The concentration of released molecules in PBS was measured with UV/Vis spectrometry. These studies showed that release of all tested dextrans (3–70 kDa) and BSA molecules occurred within 24 h in PBS (see Supporting Information). 100% of encapsulated protein was released after 20 h from PA MCs. A similar effect was observed for all dextrans, but 3–5 kDa dextran was released the fastest (after 6 h).

Using the well-known diversity of bioactivity that PA nanofibers can offer,^[25,34–37] the MCs could create a versatile platform to generate cell-like objects for many therapies. To demonstrate that more than one type of PA can be incorporated into the shell, we used FITC-labeled PA ($C_{16}V_3A_3K_3$ -FITC). We mixed $C_{16}V_3A_3K_3$ -FITC PA with $C_{16}V_3A_3K_3$ PA (1:100 w/w, total concentration 0.1 wt%) prior to spraying of 0.25 wt% alginate (Figure 3B). The membrane of these fluorescein-MCs showed a clear fluorescent edge contrast (Figure 3B), thus suggesting successful co-self-assembly of FITC-PA with PA and AL. This type of functionalization offers a straightforward approach for the incorporation of specific fluorescent tags, recognition units, and bioactive epitopes for cell signaling or cell targeting into the high surface area of these filamentous particles. Fluorescent tags may allow, for instance, in vivo tracking of MCs using imaging techniques.

We conclude that specially designed simple methods of self assembly between peptides and biopolymers can be used to form filamentous microcapsules that could support a broad range of bioactivities for novel therapies. Their potential is based on the complex fibrous architecture that this self assembly strategy produces, thus allowing release of proteins and other macromolecules through their membranes, and the display with enormous surface area of a broad diversity of biological information. The fibrous surface of MCs offers the advantage of a high surface area and the possibility to enhance binding events through molecular design of the surface filaments. The surface filaments could also incorporate catalysts or hydrophobic drugs that could be released by pH changes. PA fibers can be functionalized with fluorophores, tagged with bioactive sequences of amino acids, or linked to growth factors and bioactive biopolymers such as heparin. We propose that the biodiverse array of biological signals and efficacy of peptide amphiphiles demonstrated previously both in vitro and in vivo will allow the microcapsules to function as artificial cells in novel therapeutic strategies. The MCs described have membranes that allow them to deliver proteins and therefore similarly large macromolecules. The delivery of proteins from the internal compartment of a MC is not a common characteristic of liposomes, vesicles, or layer-by-layer microcapsules. This property is cell-mimetic in that the ability to deliver proteins from the cytoplasm to the extracellular space is one of the functions of biological cells. Cells also have recognition sites on their surfaces; this function is naturally incorporated in the fibrillar structure of our MCs. These MCs can also have sizes and morphologies that occur in natural cells, particularly a fibrous morphology. The potential for tuned permeability, size, shape, mechanical properties, and most importantly the possibility to encapsulate nanoscale compartments, cell components, and

macromolecules make these MCs excellent systems to innovate cell-mimetic functions.

Experimental Section

The peptide amphiphile ($C_{16}V_3A_3K_3$) was synthesized by using standard 9-fluorenylmethyloxycarbonyl (Fmoc) solid-phase peptide synthesis on a CS Bio automated peptide synthesizer and purified using reverse-phase HPLC (Agilent HP 1050 system) with a mobile phase gradient consisting of water and acetonitrile, each containing 0.1% v/v trifluoroacetic acid.^[28] Amino acids and Rink MBHA were purchased from Novabiochem Corporation (San Diego, CA, USA). All other reagents were purchased from Mallinckrodt (Hazelwood, MO, USA). PAs were dialyzed and isolated by lyophilization. ESI (LCQ Advantage) and MALDI-TOF-MS (Voyager DE Pro) were used to confirm mass and purity. Alginate HF120RBS (MW 300–400 kDa) was purchased from FMC Biopolymers, (G/M (%) 45–55/45–55, 1 wt%). Calcium chloride, sodium chloride, fluorescein isothiocyanate dextrans, and sodium citrate were purchased from Sigma Aldrich. FITC-BSA was purchased from Molecular Probes. Strainers with pore diameter of 40 μ m were purchased from BD Falcon.

Spraying of 0.25 wt% alginate solution was performed using Capillary PicoSpray (see the Supporting Information). The droplets of biopolymer were ejected into the aqueous solution of 0.1 wt% PAs containing 2 wt% $CaCl_2$ (for the gel-filled microcapsules). The microdroplets were passed through the strainer (pore diameter < 40 μ m). The solution of PAs was stirred continuously with a magnetic stirrer. Once the MCs were formed, they were removed from the PA solution after 15 min of incubation, passed through the strainer again, washed with MilliQ water three times, and centrifuged. Finally, the droplets were resuspended in saline solution (0.9% NaCl), PBS, or water. PA MCs were stored in saline or MilliQ water for weeks without rupturing.

Encapsulation of dextrans and BSA: FITC-labeled dextran with molecular weight of 3–5 kDa, 10 kDa, 40 kDa, and 70 kDa as well as FITC-BSA were used. Five different solutions were prepared; each solution was a mixture of 1 mgmL⁻¹ of dextran (3–5, 10, 40, and 70 kDa) and BSA with 0.5 wt% alginate. The mixture was sprayed using the Capillary PicoSpray method into a 0.1 wt% $C_{16}V_3A_3K_3$. The MCs were rinsed with MilliQ water and PBS. MCs with encapsulated dextrans and BSA (fluorescein-labeled) were imaged with a fluorescence microscope (Nikon).

Release of dextrans and BSA: The MCs were subjected to a release study in PBS (pH 7.4) at 37 °C in an incubator–shaker for 24 h. Samples of 100 μ L were taken from the release medium at specific time intervals for a total period of 24 h and were replaced with the same amount of PBS. Each sample was measured at 494 nm with a UV/Vis spectrometer (SpectraMax M5, Molecular Devices).

SEM of microcapsules: before SEM characterization the samples were dehydrated by exchange with ethanol of increasing concentration (10, 20, 30 up to 100% of ethanol). MCs were immersed in each solution for at least 10 min (e.g., 10 min in 10, 20, 30% etc., and finally in 100% ethanol). The ethanol was removed by critical point drying (CPD). Large (ca. 1 mm) liquid-core MCs were cut open with tweezers before obtaining SEM micrographs. Smaller liquid-core MCs (< 100 μ m) usually collapsed during CPD processing while gel-core MCs remain spherical shape. Osmium (8 nm) was deposited with an osmium plasma coater onto dry MCs in order to minimize electron beam charging during imaging.

Received: February 1, 2011

Published online: May 23, 2011

Keywords: amphiphiles · capsules · membranes · peptides · self-assembly

- [1] J. K. Oh, D. I. Lee, J. M. Park, *Prog. Polym. Sci.* **2009**, *34*, 1261–1282.
- [2] D. Walsh, L. Arcelli, V. Swinerd, J. Fletcher, S. Mann, *Chem. Mater.* **2007**, *19*, 503–508.
- [3] R. M. Capito, H. S. Azevedo, Y. S. Velichko, A. Mata, S. I. Stupp, *Science* **2008**, *319*, 1812–1816.
- [4] D. Carvajal, R. Bitton, J. R. Mantei, Y. S. Velichko, S. I. Stupp, K. R. Shull, *Soft Matter* **2010**, *6*, 1816–1823.
- [5] L. W. Chow, R. Bitton, M. J. Webber, D. Carvajal, K. R. Shull, A. K. Sharma, S. I. Stupp, *Biomaterials* **2011**, *32*, 1574–1582.
- [6] T. M. S. Chang, *Science* **1964**, *146*, 524–525.
- [7] G. Decher, *Science* **1997**, *277*, 1232–1237.
- [8] B. Städler, R. Chandrawati, K. Goldie, F. Caruso, *Langmuir* **2009**, *25*, 6725–6732.
- [9] D. Haložan, U. Riebentanz, M. Brumen, E. Donath, *Colloids Surf. A* **2009**, *342*, 115–121.
- [10] Q. He, L. Duan, W. Qi, K. Wang, Y. Cui, X. Yan, J. Li, *Adv. Mater.* **2008**, *20*, 2933–2937.
- [11] E. Donath, G. B. Sukhorukov, F. Caruso, S. A. Davis, H. Mohwald, *Angew. Chem.* **1998**, *110*, 2323–2327; *Angew. Chem. Int. Ed.* **1998**, *37*, 2201–2205.
- [12] F. Caruso, R. A. Caruso, H. Mohwald, *Science* **1998**, *282*, 1111–1114.
- [13] Q. He, Y. Cui, J. Li, *Chem. Soc. Rev.* **2009**, *38*, 2292–2303.
- [14] E. Kamio, S. Yonemura, T. Ono, H. Yoshizawa, *Langmuir* **2008**, *24*, 13287–13298.
- [15] H. Uludag, P. De Vos, P. A. Tresco, *Adv. Drug Delivery Rev.* **2000**, *42*, 29–64.
- [16] H. Gin, B. Dupuy, C. Baquey, D. Ducassou, J. Aubertin, *J. Microencapsulation* **1987**, *4*, 239–242.
- [17] S. S. Dhumal, A. K. Suresh, *Polymer* **2010**, *51*, 1176–1190.
- [18] W. S. Yin, M. Z. Yates, *J. Colloid Interface Sci.* **2009**, *336*, 155–161.
- [19] D. X. Li, Y. K. Oh, S. J. Lim, J. O. Kim, H. J. Yang, J. H. Sung, C. S. Yong, H. G. Choi, *Int. J. Pharm.* **2008**, *355*, 277–284.
- [20] C. Y. Yu, W. Wang, H. Yao, H. J. Liu, *Drying Technol.* **2007**, *25*, 695–702.
- [21] C. Priest, A. Quinn, A. Postma, A. N. Zelikin, J. Ralston, F. Caruso, *Lab Chip* **2008**, *8*, 2182–2187.
- [22] P. J. A. Kenis, R. F. Ismagilov, G. M. Whitesides, *Science* **1999**, *285*, 83–85.
- [23] A. S. Utada, E. Lorenceau, D. R. Link, P. D. Kaplan, H. A. Stone, D. A. Weitz, *Science* **2005**, *308*, 537–541.
- [24] K. S. Huang, M. K. Liu, C. H. Wu, Y. T. Yen, Y. C. Lin, *J. Micromech. Microeng.* **2007**, *17*, 1428–1434.
- [25] G. A. Silva, C. Czeisler, K. L. Niece, E. Beniash, D. A. Harrington, J. A. Kessler, S. I. Stupp, *Science* **2004**, *303*, 1352–1355.
- [26] K. Rajangam, H. A. Behanna, M. J. Hui, X. Q. Han, J. F. Hulvat, J. W. Lomasney, S. I. Stupp, *Nano Lett.* **2006**, *6*, 2086–2090.
- [27] H. Storrie, M. O. Guler, S. N. Abu-Amara, T. Volberg, M. Rao, B. Geiger, S. I. Stupp, *Biomaterials* **2007**, *28*, 4608–4618.
- [28] M. J. Webber, J. Tongers, M. A. Renault, J. G. Roncalli, D. W. Losordo, S. I. Stupp, *Acta Biomater.* **2010**, *6*, 3–11.
- [29] R. N. Shah, N. A. Shah, M. M. D. Lim, C. Hsieh, G. Nuber, S. I. Stupp, *Proc. Natl. Acad. Sci. USA* **2010**, *107*, 3293–3298.
- [30] A. Mata, Y. B. Geng, K. J. Henrikson, C. Aparicio, S. R. Stock, R. L. Satcher, S. I. Stupp, *Biomaterials* **2010**, *31*, 6004–6012.
- [31] J. C. Stendahl, L. J. Wang, L. W. Chow, D. B. Kaufman, S. I. Stupp, *Transplantation* **2008**, *86*, 478–481.
- [32] V. Sahni, A. Mukhopadhyay, V. Tysseling, A. Hebert, D. Birch, T. L. McGuire, S. I. Stupp, J. A. Kessler, *J. Neurosci.* **2007**, *30*, 1839–1855.
- [33] M. J. Webber, J. A. Kessler, S. I. Stupp, *J. Intern. Med.* **2010**, *267*, 71–88.
- [34] J. D. Hartgerink, E. Beniash, S. I. Stupp, *Science* **2001**, *294*, 1684–1688.
- [35] J. D. Hartgerink, E. Beniash, S. I. Stupp, *Proc. Natl. Acad. Sci. USA* **2002**, *99*, 5133–5138.
- [36] M. O. Guler, L. Hsu, S. Soukasene, D. A. Harrington, J. F. Hulvat, S. I. Stupp, *Biomacromolecules* **2006**, *7*, 1855–1863.
- [37] E. T. Pashuck, H. Cui, S. I. Stupp, *J. Am. Chem. Soc.* **2010**, *132*, 6041–6046.